NeuroImage: Clinical 30 (2021) 102666

Contents lists available at ScienceDirect

NeuroImage: Clinical

journal homepage: www.elsevier.com/locate/ynicl

Neurobiological substrates of the positive formal thought disorder in schizophrenia revealed by seed connectome-based predictive modeling

Ji Chen [a,b,c], Tobias Wensing [d,e], Felix Hoffstaedter [b,c], Edna C. Cieslik [b,c], Veronika I. Müller [b,c], Kaustubh R. Patil [b,c], André Aleman [f], Birgit Derntl [g], Oliver Gruber [h], Renaud Jardri [i], Lydia Kogler [g], Iris E. Sommer [j], Simon B. Eickhoff [b,c], Thomas Nickl-Jockschat [k,l,*]

[a] Department of Psychology and Behavioral Sciences, Zhejiang University, Hangzhou, China
[b] Institute of Neuroscience and Medicine, Brain & Behaviour (INM-7), Research Centre Jülich, Jülich, Germany
[c] Institute of Systems Neuroscience, Medical Faculty, Heinrich Heine University Düsseldorf, Düsseldorf, Germany
[d] Department of Psychiatry, Psychotherapy and Psychosomatics, Medical Faculty, RWTH, Aachen, Germany
[e] JARA Translational Brain Medicine, Aachen, Germany
[f] Department of Neuroscience, University of Groningen, University Medical Center Groningen, the Netherlands
[g] Department of Psychiatry and Psychotherapy, Medical School, University of Tübingen, Germany
[h] Section for Experimental Psychopathology and Neuroimaging, Department of General Psychiatry, Heidelberg University, Germany
[i] Univ Lille, INSERM U1172, Lille Neuroscience & Cognition Centre, Plasticity &SubjectivitY Team & CHU Lille, Fontan Hospital, CURE Platform, Lille, France
[j] Department of Biomedical Science of Cells and Systems, University of Groningen, University Medical Center Groningen, the Netherlands
[k] Iowa Neuroscience Institute, Carver College of Medicine, University of Iowa, Iowa City, IA, United States
[l] Department of Psychiatry, Carver College of Medicine, University of Iowa, Iowa City, IA, United States

ARTICLE INFO

Keywords:
Formal thought disorder
Neuroimaging
Machine learning

ABSTRACT

Formal thought disorder (FTD) is a core symptom cluster of schizophrenia, but its neurobiological substrates remain poorly understood. Here we collected resting-state fMRI data from 276 subjects at seven sites and employed machine-learning to investigate the neurobiological correlates of FTD along positive and negative symptom dimensions in schizophrenia. Three a priori, *meta*-analytically defined FTD-related brain regions were used as seeds to generate whole-brain resting-state functional connectivity (rsFC) maps, which were then compared between schizophrenia patients and controls. A repeated cross-validation procedure was realized within the patient group to identify clusters whose rsFC patterns to the seeds were repeatedly observed as significantly associated with specific FTD dimensions. These repeatedly identified clusters (i.e., robust clusters) were functionally characterized and the rsFC patterns were used for predictive modeling to investigate predictive capacities for individual FTD dimensional-scores. Compared with controls, differential rsFC was found in patients in fronto-temporo-thalamic regions. Our cross-validation procedure revealed significant clusters only when assessing the seed-to-whole-brain rsFC patterns associated with positive-FTD. RsFC patterns of three fronto-temporal clusters, associated with higher-order cognitive processes (e.g., executive functions), specifically predicted individual positive-FTD scores ($p = 0.005$), but not other positive symptoms, and the PANSS general psychopathology subscale ($p > 0.05$). The prediction of positive-FTD was moreover generalized to an independent dataset ($p = 0.013$). Our study has identified neurobiological correlates of positive FTD in schizophrenia in a network associated with higher-order cognitive functions, suggesting a dysexecutive contribution to FTD in schizophrenia. We regard our findings as robust, as they allow a prediction of individual-level symptom severity.

1. Introduction

Formal thought disorder (FTD) is characterized by disorganized and incoherent speech and can manifest in various disorders (Andreasen, 1979; DeLisi, 2001). In particular, FTD is a core symptom of schizophrenia, defined by the DSM-5 as one of the five major diagnostic

* Corresponding author at: Department of Psychiatry, Iowa Neuroscience Institute, University of Iowa, 2312 Pappajohn Biomedical Discovery Building, Iowa City 52242, IA, United States.
E-mail address: thomas-nickl-jockschat@uiowa.edu (T. Nickl-Jockschat).

https://doi.org/10.1016/j.nicl.2021.102666
Received 14 July 2020; Received in revised form 1 April 2021; Accepted 3 April 2021

criteria. Critical for the disease trajectory, FTD serves as a robust and consistent predictor of transition to psychosis in clinical high-risk samples (Hartmann, 2016; DeVylder et al., 2014; Armando et al., 2015). The clinical presentation of FTD is heterogeneous: impairments as diverse as impoverished thinking, disorganized thought processes or lack of spontaneous conversation are usually subsumed under this broad umbrella (Kircher et al., 2018). Given this heterogeneity, researchers have suggested a dichotomy that relates to the concept of positive and negative symptoms in schizophrenia (Andreasen et al., 1990). Following this line of thought, disorganized thinking would be regarded as "positive FTD", while impoverished thought processes would be labeled as "negative FTD" (Kircher et al., 2018; Andreasen, 1986). This dichotomy appears to be clinically highly relevant (Roche et al., 2015), since the negative FTD dimension has been shown to better predict conversion to schizophrenia in subjects at risk for psychosis, irrespective of genetic liability (Ott et al., 2002). Also, these two symptom clusters of FTD relate to distinct neuropsychological deficits (Nagels, 2016). Moreover, specific FTD dimensions (i.e., negative or positive FTD), rather than overall FTD, were found to be associated with poor outcome in psychotic disorders (Roche et al., 2015; Roche, 2016). Hence, separating FTD into positive and negative dimensions and investigating their respective neurobiological underpinnings is important for understanding schizophrenia.

Early functional magnetic resonance imaging (fMRI) studies mainly compared regional neural activations between schizophrenia patients and healthy controls during different language-related tasks and examined FTD symptoms as a single dimension (McGuire et al., 2002; Ragland, 2008; Kircher, 2003; Arcuri et al., 2012; Chen et al., 2014; Cavelti et al., 2018). While abnormal activations within the traditional temporal language network (Friederici, 2012) were consistently observed and reported to be correlated with FTD severity in schizophrenia (Cavelti et al., 2018); findings outside this language network including prefrontal, postcentral (Kircher, 2001), and fusiform gyri (Ragland, 2008; Kircher et al., 2008) were less frequently implicated. A recent *meta*-analysis from our lab identified three clusters within the temporal lobe, mainly associated with language functions, indicating convergent aberrant neural activations associated with FTD (Wensing, 2017). These results support the notion that abnormalities in language-processing related brain regions and networks underlie FTD symptoms in schizophrenia (i.e., the "dyssemantic hypothesis") (Goldberg et al., 1998); but do not allow to conclude whether FTD also relates to deficits in circuits involved in higher-order cognitive processes ("dysexecutive hypothesis") (Barrera et al., 2005). Furthermore, the use of a generic concept of FTD entails pooling over heterogeneous symptoms, while the relatively small number of fMRI studies, which investigated the neurobiological correlates separately for positive and negative FTD dimensions, suggested distinct pathophysiological processes. Interestingly, altered neural activation in the inferior frontal cortex (McGuire et al., 2002; Arcuri et al., 2012; Kircher, 2001); as well as reduced activity and grey matter volume in Wernicke's area have been implicated in positive FTD (McGuire et al., 2002; Kircher, 2001a, 2001b). Negative FTD, in turn, was reported to be associated with abnormalities in dorso-prefrontal and parietal regions involving executive and cognitive control processes (Kircher, 2003; McGuire, 1998; Fuentes-Claramonte et al., 2020). Nevertheless, neural findings for specific FTD dimensions from these small sample studies require a follow-up in larger cohorts of schizophrenia patients. On the other hand, region-based approaches would fall short to detect dysconnection as an important pathophysiological component that presumably underlies schizophrenia symptomatology (Pettersson-Yeo et al., 2011; Uhlhaas, 2013; Dong, 2018). Connectivity-based analyses might also help to gain further insight into the controversy regarding a dyssemantic (Goldberg et al., 1998) vs. dysexecutive (Barrera et al., 2005) pathogenesis of FTD symptom dimensions.

Resting-state functional connectivity (rsFC) allows to study brain organization at the level of synchronized spontaneous neural activity (Fox and Raichle, 2007). Importantly, schizophrenia patients show pronounced neurobiological abnormalities concerning intrinsic connectivity patterns between widespread brain regions and networks (Pettersson-Yeo et al., 2011; Uhlhaas, 2013; Dong, 2018). However, rsFC-based studies on FTD in schizophrenia are scarce and previous results remain inconsistent (Liemburg, 2012; Skudlarski, 2010). Also the interpretation of prior seed-based rsFC analyses on the revealed circuit-level neural pathophysiology is likewise varying due to the different choices of seed regions (Liemburg, 2012; Skudlarski, 2010) In contrast, a definition of seeds based on regions identified by *meta*-analyses as showing convergent aberrant activation associated with FTD facilitates the identification of FTD-related circuit-level neural pathophysiology with improved functional specificity and therefore interpretability. This is because these regions were identified based on prior task-fMRI studies, representing robust and the most likely brain locations associating with FTD across many subjects and variations in paradigm (Laird, 2009; Eickhoff et al., 2012). Moreover, correlations found in previous studies were based on univariate group-level analyses on small and geographically restricted samples, raising doubts over the reproducibility and robustness. Multivariable predictive modeling with cross-validation on multi-site data, in contrast, could not only allow for identifying a robust neurobiological substrate of FTD, but for assessing the predictability of the identified neurobiological patterns for individual FTD severity.

In the present study, we used as seeds the clusters yielded by our prior *meta*-analysis (Wensing, 2017). These clusters were identified as robustly associated with aberrant neural processes engaged during 55 different, but functionally related experiments across 18 prior task-based fMRI studies on FTD. Based on these robust clusters, we aimed to identify whole-brain dysconnectivity associated with FTD by generating seed-to-whole-brain rsFC maps and comparing them between a multi-site schizophrenia sample and matched healthy subjects. Importantly, we realized a cross-validation-based feature selection to derive robust rsFC associative patterns for not only the overall FTD, but also the positive and negative FTD dimensions assessed by the items taken from the well-established *"Positive and Negative Syndrome Scale"* (PANSS) (Kay et al., 1987). Furthermore, the identified robust seed-to-whole-brain rsFC patterns were employed as features for predictive modeling to assess their predictive capacity for individual FTD severity in out-of-sample data. Finally, regions with connectivity patterns robustly associated with FTD were functionally characterized to reveal their neurocognitive functions (Laird, 2009; Genon et al., 2018). We hypothesized that 1) differential seed-to-whole-brain rsFC patterns are present in schizophrenia patients compared to healthy controls; 2) the positive, negative, and composite FTD symptom dimensions would be associated with differential rsFC patterns in schizophrenia; 3) the identified robust neurobiological profile of FTD would allow for out-of-sample prediction of individual FTD dimension scores and involves regions related to higher-order cognitive functions.

2. Materials and methods

2.1. Sample

We jointly investigated 276 subjects recruited from seven sites. In detail, a total of 121 DSM-IV diagnosed schizophrenia patients and 121 healthy controls from five independent medical centers located in Europe (Aachen-1, Göttingen, Groningen and Utrecht) and the USA (Albuquerque, NM; i.e., the COBRE sample; 80% of the subjects initially enrolled [COBRE#1]) were included as the main sample (Table 1 & Supplementary material S1). Within each site, patients and controls were matched for age, gender (Supplementary Table 1), and head motion during scans (root mean-square [RMS] movement and DVARS [temporal derivative of the RMS of the fMRI time series across voxels][39]) (all $p > 0.05$) (Supplementary Table 2). These demographic and movement variables did not differ significantly between the two groups

Table 1
Clinical characteristics of schizophrenia patients in the main sample.

	Aachen-1	Albuquerque (COBRE#1)	Göttingen	Groningen	Utrecht	Total	*P*-value[1]
N	13	51	27	20	10	121	
Illness duration	8.08 ± 8.66	15.54 ± 12.64	6.67 ± 7.69	9.60 ± 10.46	5.11 ± 5.30	11.03 ± 11.16	0.002
Antipsychotic treatment							
FGA	0	3	1	2	1	7	
SGA	13	43	19	8	4	87	
FGA + SGA	0	2	5	0	0	7	
Missing	0	3	2	10	5	20	
OZP-equivalent[2]	21.72 ± 10.05	14.84 ± 10.96	25.06 ± 11.49	14.55 ± 8.31	17.10 ± 12.42	18.81 ± 11.60	0.001
PANSS							
FTD composite	4 (4–9)	8 (5–14)	7 (4–14)	6 (4–14)	10 (6–14)	7 (4–14)	≤0.001
FTD positive (P2 item)	1 (1–4)	1 (1–5)	2 (1–5)	1 (1–4)	2 (1–4)	1 (1–5)	0.025
FTD negative (items N5 + N6 + N7)	3 (3–6)	6 (3–13)	5 (3–9)	4 (3–10)	7 (4–11)	5 (3–13)	≤0.001
Positive	14.54 ± 7.08	14.35 ± 4.45	11.67 ± 3.23	14.74 ± 5.30	17.44 ± 2.96	14.06 ± 4.80	0.016
Negative	9.85 ± 4.04	15.12 ± 5.25	13.04 ± 4.40	13.21 ± 4.45	15.33 ± 4.56	13.78 ± 4.99	0.007
General	24.15 ± 5.66	29.41 ± 8.12	27.81 ± 5.93	27.00 ± 8.97	31.33 ± 8.70	28.26 ± 7.71	0.145
Total	**48.54 ± 14.64**	**58.88 ± 13.36**	**52.52 ± 10.00**	**52.11 ± 18.28**	**64.11 ± 13.82**	**55.62 ± 14.25**	**0.019**

Note: Data are mean ± SD or median (range). N, number of subjects per research site; FGA, first-generation antipsychotic; SGA, second-generation antipsychotic; PANSS, Positive and Negative Symptom Scale; FTD, formal thought disorder; OZP, olanzapine. [1]Statistical comparison between sites was conducted using either one-way analysis of variance (ANOVA) or Kruskal-Wallis test where appropriate. [2]Dosage in mg/day.

across all sites ($p > 0.05$). Duration of disease differed significantly between sites ($p = 0.002$). An independent dataset ($N = 34$), including the COBRE#2 sample (the 20% remaining patients that were not enclosed in the main sample), as well as nine DSM-IV-TR and nine ICD-10 diagnosed schizophrenia patients from two new sites of Lille and Aachen-2 (Supplementary Table 3), were used for external validation of the predictive models. The main and the validation samples were comparable in demographic variables (all $p > 0.05$). For each site, subjects gave fully written informed consent and study approval was given by the respective ethics committees/insitutional review boards. Additional approval to pool and re-analyze data was provided by the ethics committee of the RWTH Aachen University, Aachen, Germany.

2.2. Clinical characteristics

Severity of psychopathology was assessed using the PANSS (Table 1 and Supplementary Table 3). Four PANSS items, "conceptual disorganization" (P2), "difficulty in abstract thinking" (N5), "lack of spontaneity and flow of conversation" (N6) and "stereotyped thinking" (N7) were used for assessing the FTD symptoms (Chen et al., 2014; Horn et al., 2010; Nagels, 2012). Although no definite consensus exists on the exact set of PANSS items to assess FTD in schizophrenia, we have chosen the most consistently selected items from the literature (Chen et al., 2014; Horn et al., 2010; Nagels, 2012; Tan et al., 2014). Of note, this choice allowed us to differentiate between the positive and negative symptom dimension of FTD, which was a major goal of this study. Specifically, according to their definitions (i.e., belonging to positive or negative symptoms in schizophrenia) in the PANSS, the item P2, which measures disruption of goal-directed sequencing (manifested as circumstantiality, tangentiality, loose associations, or illogicality), was used to assess the severity of positive FTD. The items N5 (impairment in the use of the abstract-symbolic mode of thinking), N6 (reduced fluidity and productivity of the verbal-interactional process) and N7 (expressed as rigid, repetitious, or barren thought content) were subsumed under "negative FTD" (Horn et al., 2010; Nagels, 2012), defining the FTD dimensions as a dichotomous structure as suggested by *Andreasen* (Andreasen, 1979). The composite score was calculated as the sum scores of the positive and the negative FTD items (i.e., P2, N5, N6, N7). Patients in the validation dataset showed more severe FTD symptoms than those in the main sample ($p < 0.001$), which would help to indicate the sensitivity of our predictive modeling. Dosages of current antipsychotic medication were transformed into olanzapine equivalents (Gardner et al., 2010).

2.3. Definition of seed regions

We used as seeds three left-lateralized clusters that were identified by a previous coordinate-based activation likelihood estimation (ALE) (Eickhoff et al., 2012) *meta*-analysis on functional brain correlates of FTD (Wensing, 2017). These clusters were located in the superior temporal gyrus (STG) (110 voxels, volume: 880 mm^3), the dorsal posterior middle temporal gyrus (dpMTG) (109 voxels; volume: 872 mm^3), and the ventral posterior (vp)MTG (71 voxels; volume: 568 mm^3) (Fig. 1A).

2.4. FMRI data acquisition and preprocessing

All datasets were scanned (Supplementary Tables 4 & 5) and preprocessed using SPM8 (http://www.fil.ion.ucl.ac.uk/spm) and the FMRIB's independent component analysis (ICA)-based X-noiseifier (FIX) for denoising the fMRI data (Salimi-Khorshidi et al., 2014; Griffanti et al., 2014; Liu et al., 2020) (http://fsl.fmrib.ox.ac.uk/fsl/fslwiki/FSL) (Supplementary material S2.1). One subject in the control group and two subjects in the patient group (main sample) showed excessive head movement of DVARS > 5 and were, hence, excluded from subsequent analyses. The threshold of DVARS = 5 is roughly equivalent to a framewise displacement of 0.5 mm (Power et al., 2012); which has been commonly used in the literature (Power et al., 2015) and was employed in our prior work with similar patient cohorts (Chen, 2020, 2021). Within the patient group, age and duration of disease did not correlate with any FTD dimension. FTD dimensional-scores did not differ between male and female patients (all $p > 0.05$). Head motion (DVARS) significantly differed between sites ($p < 0.001$, one-way ANOVA), but was not significantly correlated with the scores for any FTD dimensions after adjusting for age/gender/site effects (all p-values > 0.09). Nevertheless, to avoid any (possible) contributions of head motion to the prediction of individual FTD dimension scores, head motion effects were adjusted in our predictive modeling (Dubois, 2018; Smith and Nichols, 2018). We regressed out white matter and CSF signals from the overall time-series, but not the global mean signals, since global signal removal (GSR) is still controversial in preprocessing (Murphy and Fox, 2017) and a previous study showed that GSR would obscure an effect predictive of symptoms in schizophrenia patients (Yang et al., 2014). Seed to whole-brain rsFC maps were generated by calculating the Fisher's z-transformed linear Pearson correlations between the first eigenvariate of the seed time-series and the time-series of all other grey matter voxels of the entire brain (Kraguljac, 2017).

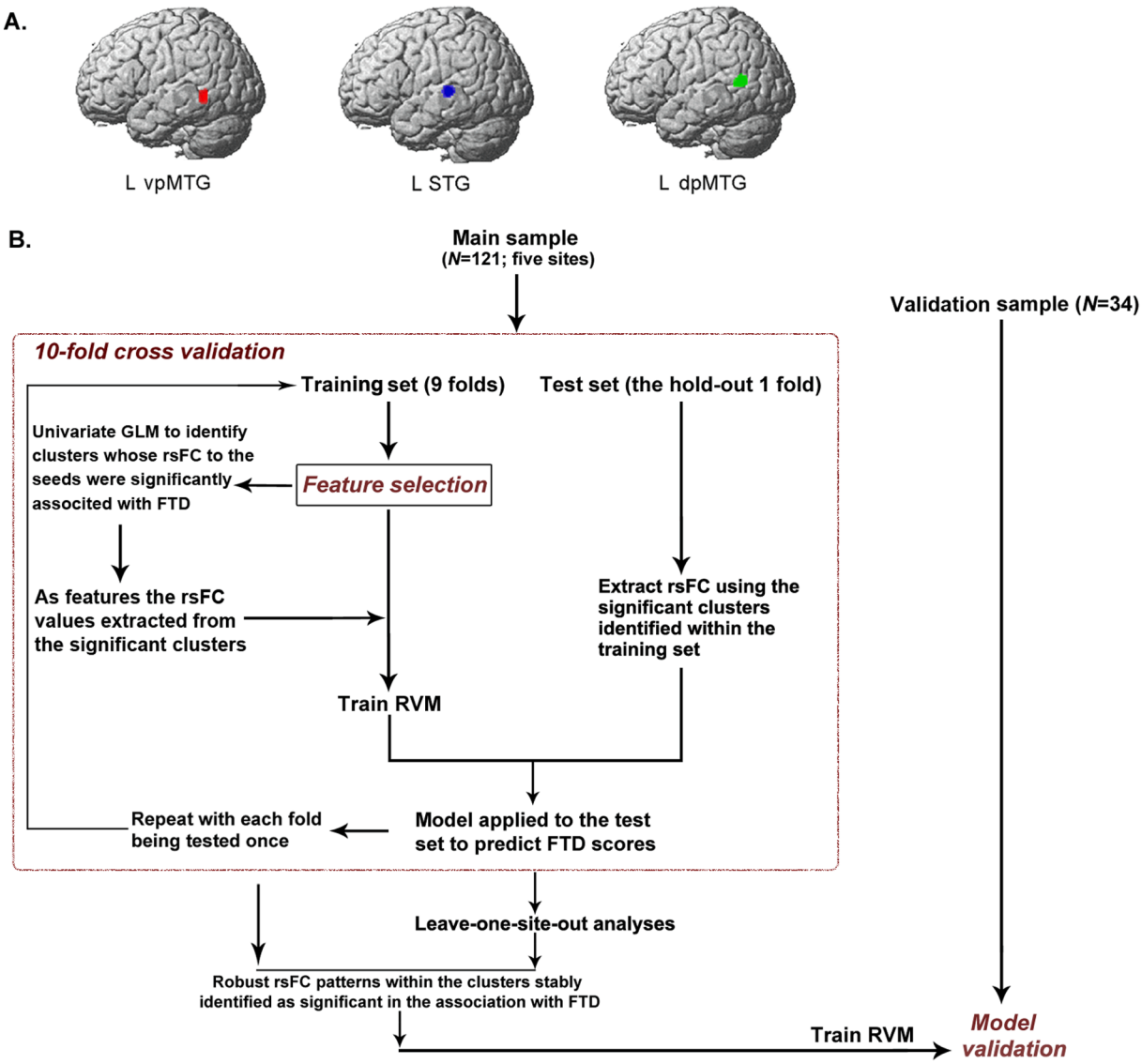

Fig. 1. Seed regions used for functional connectivity map construction and illustration of the overall feature selection and multivariable predictive modeling procedure. A) We used three clusters as seeds that showed consistently aberrant activation associated with FTD in our previous activation likelihood estimation based *meta*-analysis (Wensing, 2017). MNI coordinates: left superior temporal gyrus (STG; −54, −28, 4); ventral posterior middle temporal gyrus (vpMTG; −46, −50, 22); and dorsal posterior MTG (dpMTG; −56, −56, 12). B) Flowchart illustrates the identification of rsFC patterns that were robustly associated with FTD specific dimensions, and the use of the identified rsFC as features for predictive modeling. GLM, general linear model; RVM, relevance vector machine; rsFC, resting-state functional connectivity; FTD, formal thought disorder.

2.5. Between-group comparison of seed-to-whole-brain rsFC

A general linear model (GLM) was constructed for each of the seed regions by including group (schizophrenia vs. controls) as a categorical variable to identify voxels that were differentially connected to the seed regions in schizophrenia patients compared to healthy controls. Effects of age, gender, site, and head motion (DVARS) were controlled within the GLMs. The resulting statistical maps were thresholded at cluster-level family-wise error corrected $p < 0.05$ (cluster-forming threshold $p < 0.001$) according to the random field theory (RFT).

2.6. Identification of robust rsFC correlates of FTD through repeated cross-validation and multivariable predictive modeling: Predicting individual FTD dimension scores

We, next, implemented a 10-fold cross-validation procedure to identify robust seed-to-whole-brain rsFC correlates of FTD (composite, negative, and positive) dimensions and the process was nested within predictive modeling to test the predictive capacity of the identified rsFC patterns for individual FTD dimensional-scores in out-of-sample data. We deliberately chose a supervised feature-extraction procedure in predictive modeling, as the identification of seed-to-whole-brain rsFC patterns robustly associated with FTD was our main aim. In each 10-fold process, the original sample was randomly divided into ten equal-sized groups and each of the groups (i.e., the test sample) was predicted once. Hence, there were ten training samples with 8/9 patients shared. This resembles a ten times repeated subsampling procedure, during which 90% subjects are randomly drawn from the original data without replacement. Basically, if there are rsFC patterns stably and repeatedly detected as significantly associated with FTD irrespective of data perturbation, these patterns can be reasonably regarded as robust. The whole procedure can be parsed into three steps (Fig. 1B):

i) Identification of rsFC patterns significantly associated with FTD within the training samples

Within each training sample, three univariate GLMs (one for each seed) were constructed to identify significant clusters with rsFC to the seeds significantly associated with FTD dimensional scores after controlling for age, gender, site, and head motion effects. Statistical maps were corrected for multiple comparisons by using the same RFT approach described above. This is also critical for predictive modeling to avoid test-to-training information leakage (Dubois, 2018; Shen, 2017).

ii) Feature extraction

Significant clusters were then used as masks to determine the voxel positions where the *Fisher's* z-transformed rsFC values were extracted for both the training and the test samples. The extracted voxel-wise rsFC values were averaged over the voxels within each significant cluster. The mean rsFC values for all of the detected significant clusters were used as features for predictive modeling. This supervised feature selection strategy resembles "connectome-based predictive modeling" (CPM) (Shen, 2017); as a long-standing feature selection method described in machine learning literature (Guyon and Elisseeff, 2003; Kohavi and John, 1997); which could effectively improve predictive performance while discarding irrelevant variables (Finn et al., 2015; Beaty et al., 2018; Rosenberg et al., 2016).

iii) Predictive modeling

Since the extracted rsFC values were the original Fisher's z-transformed values, i.e., not de-confounded, a confound-adjustment procedure was performed prior to predictive modeling to control for confounding effects that may contribute to the predictions. More specifically, in keeping with the recommended strategy (Pervaiz et al., 2020); confounding effects of age, gender, site and head motion (DVARS) on both the extracted features and the FTD dimensional scores were adjusted. To avoid data leakage within cross-validation (Dubois, 2018; Snoek et al., 2019), confound-adjustment was conducted by learning the confound regression models within the training-set and applying the regression weights to both the training and the test sets to obtain confound-adjusted training and test sets (Dubois, 2018; Snoek et al., 2019; More et al., 2020). Then, a relevance vector machine (RVM) (Tipping, 2001) (Supplementary material S2.2.1) was employed to realize multivariable regression through probabilistic Bayesian learning. That is, within the training-set, the confound-adjusted rsFC features were fed into RVM model training with confound-adjusted FTD dimension scores as the target variable. Then, RVM weights from the trained model were applied to the confound-adjusted rsFC features in the test-set to obtain the predicted FTD dimensional-scores for out-of-sample data.

The folds were stratified to ensure the proportion of patients between sites in each fold was (approximately) equal to that in the entire sample, rendering the inclusion of sites in training and test sets balanced. Holding out each of the ten groups once in the process allowed to generate a probability map to denote how many times the significant clusters were identified, and to evaluate the prediction performance across the entire data set by computing the *Pearson's* correlation coefficient and the normalized root-mean-square-error (nRMSE) between the (confound-adjusted) FTD dimensional-scores and their out-of-sample predictions. To ensure a reliable estimation, the 10-fold process described above was repeated 50 times using random initial splits of the data. The obtained correlation coefficients and nRMSE values were averaged over the all repetitions, and the clusters identified as significantly associated with FTD dimensions were accumulated (maximal selection number = 500). Clusters with a higher selection number refer to more robustly associated given rsFC patterns with FTD.

A leave-one-site-out (LOSO) cross-validation analysis was followed to assess the generalization performance across sites (Supplementary material S2.2.2). The resulting five correlation coefficients and nRMSE values were averaged. We also pooled the predicted (confound-adjusted) FTD dimensional-scores from the left-out sites and then correlated them with the actual (confound-adjusted) scores. Of note, the folds in 10-fold cross-validation and the sites in LOSO analysis were not independent of each other and, hence, using parametric statistics to assess the cross-validated performance is problematic (Noirhomme, 2014). Here, significance of the 10-fold and LOSO cross-validation-based correlations against chance was assessed through permutation testing (Dubois, 2018; Combrisson and Jerbi, 2015) by shuffling the FTD dimensional scores for 5000 times while keeping everything else exactly the same (Supplementary material S2.2.3; lowest $p = 0.0002$, right-tailed). We also applied the same permutation testing to the nRMSE metric for assessing the significance of cross-validated prediction. The LOSO analysis further allowed to plot prediction accuracy (because the Pearson correlation coefficient is sample-size dependent (Yarkoni, 2009), here we used nRMSE) for each of the left-out sites as a function of sample size (i.e., number of patients).

Finally, we tested the predictability of the robust rsFC patterns identified (only) within the main sample for individual FTD dimensional-scores in an independent sample (Supplementary material S2.2.4) to avoid potential circularity, as discussed previously (Kriegeskorte et al., 2009). Briefly, clusters that were repeatedly identified as significantly associated with FTD specific dimensions within the main sample through 10-fold cross-validation and LOSO analyses were used as masks to extract the seed-to-cluster rsFC patterns for both the main and the validation samples. Effects of age, gender, site, and head motion were adjusted accordingly. Then, the RVM model trained within the main sample was applied to the validation sample to derive the predicted FTD dimensional-scores. Prediction performance was evaluated as described above. Significance of the correlation was determined by parametric statistical tests.

In addition, control analyses were performed in predictive modeling by including olanzapine-equivalent dosage as confounder. To test for the specificity of FTD-associated rsFC patterns in the prediction of FTD dimensions, the model trained based on the rsFC patterns that significantly associated with FTD was used for an analysis to predict other positive symptoms of hallucinations as well as the overall symptom severity (i.e., total PANSS score). Given the fact that our FIX-based denoising step in the preprocessing of the resting-state data has used matching training data (i.e., weights) supplied by FIX to classify noise components rather than training the weights based on our own samples due to the small sample size per site, we repeated our predictive modeling analyses by using rsFC maps generated from the images preprocessed using another ICA-based approach Automatic Removal of Motion Artifacts (ICA-AROMA) (Pruim et al., 2015; Ciric et al., 2018; Parkes et al., 2018) which does not require classifier re-training for denoising (instead of ICA-FIX). Finally, an unsupervised approach was applied to supplement our supervised feature selection method as elaborated above. In the unsupervised feature selection method, there was no relatedness between the selection of features and the target variable to be predicted, where we tested for whether the rsFC between the seeds and their significantly connected regions could predict the scores of specific FTD dimensions out-of-sample (details in Supplementary material S2.2.5).

2.7. Functional characterization of the identified brain regions

To characterize the associated functional properties of the identified clusters showing differential rsFC patterns with the three seeds in between-group comparisons and the clusters whose rsFC to the seeds robustly associated with FTD dimensions in patients, we conducted a functional characterization by implementing quantitative "forward inference" and "reverse inference" (Cieslik, 2012; Clos et al., 2013; Genon, 2017) (Supplementary material S2.3) on the sorted "behavioral domain" and "paradigm class" *meta*-data in the BrainMap database (Laird, 2009) (http://brainmap.org/) as collected from prior task-fMRI studies.

3. Results

3.1. Differential rsFC patterns in schizophrenia patients compared to healthy controls

For the left STG seed, we found decreased rsFC for schizophrenia patients compared to healthy controls with one cluster mainly encompassing the left fusiform gyrus and another one located in the left anterior MTG. Increased rsFC with this seed was found for a cluster in the right superior medial frontal gyrus (Fig. 2A, Supplementary Table 6). For the left dpMTG seed, we found one cluster indicating hyperconnectivity in schizophrenia patients compared to healthy controls in the bilateral dorsal thalamus (Fig. 2B, Supplementary Table 6). We did not find any significant between-group differences for the left vpMTG seed.

3.2. Robust rsFC correlates of FTD dimensions and their predictability in individual FTD dimensional scores

3.2.1. Identification of clusters with rsFC to the seeds that are robustly associated with FTD dimensions

Significant clusters associated with the negative and the composite FTD scores were too few (i.e., in no>5% of the in total 500 training samples within the repeated 10-fold cross-validation) for each seed region to be considered as robust and hence, were not included in subsequent predictive modeling analyses. In contrast, multiple significant clusters were identified for the positive FTD dimension. For each seed and each 10-fold cross-validation, significant clusters were accumulated to illustrate how robust the rsFC between these clusters and a particular seed relates to the severity of positive FTD. Clusters more frequently detected as significantly associated with positive-FTD in the repeated 10-fold process were considered as more robust (Fig. 3A). As aforementioned, clusters identified as significant in<5% of the in total 500 training samples within the 50 times repeated 10-fold cross-validation were discarded due to being regarded as too unstable. Clusters located in the right dorso-prefrontal region (mainly middle frontal gyrus [MFG]) were more frequently detected as significantly associated with the positive-FTD in the repeated 10-fold process than two clusters that were located in the right inferior temporal cortex and the supramarginal gyrus. RsFC of these clusters to the left STG seed was co-varying negatively with the positive-FTD (Fig. 3A). For the left dpMTG seed, clusters located in the right MTG were identified as showing significant positive associations with the positive FTD dimension scores. RsFC between the clusters stretching across the right inferior parietal lobule (IPL) and the left vpMTG seed was found to robustly and negatively associate with the positive FTD dimension in 491 out of the overall 500 training samples.

3.2.2. Features and predictive modeling

Within each cross-validation, significant rsFC patterns for the three seeds identified in the training samples were combined to construct the feature space for RVM model training within the training samples to predict individual positive FTD scores in the test samples. The predicted (confound-adjusted) positive FTD scores showed a significant above-chance positive correlation with the actual (confound-adjusted) scores ($r = 0.30$, $p = 0.0048$; $nRMSE = 0.97$, $p = 0.0060$; after excluding a suspected outlier of predicted score: $r = 0.25$, $p = 0.0168$; $nRMSE = 0.99$, $p = 0.0350$; Fig. 3B). Outliers (i.e., the unusual predicted FTD scores) were identified first by visual inspection and, second, by calculating the standardized residuals (Altman and Krzywinski, 2016). For the latter approach, predicted scores with a standardized residual > 3 (in absolute value) were regarded as outliers, based on a commonly used cutoff in literature (Guo et al., 2015; Lehmann, 2013). This approach was applied, because outlier values may optimistically bias the estimation of the correlation between the observed FTD scores and their predictions.

LOSO analysis corroborated the 10-fold results ($r = 0.32$, averaged over the left-out sites; correlation after pooling the left-out sites: $r = 0.26$, $p = 0.0034$; $nRMSE = 0.99$, $p = 0.0024$ [the significance held after

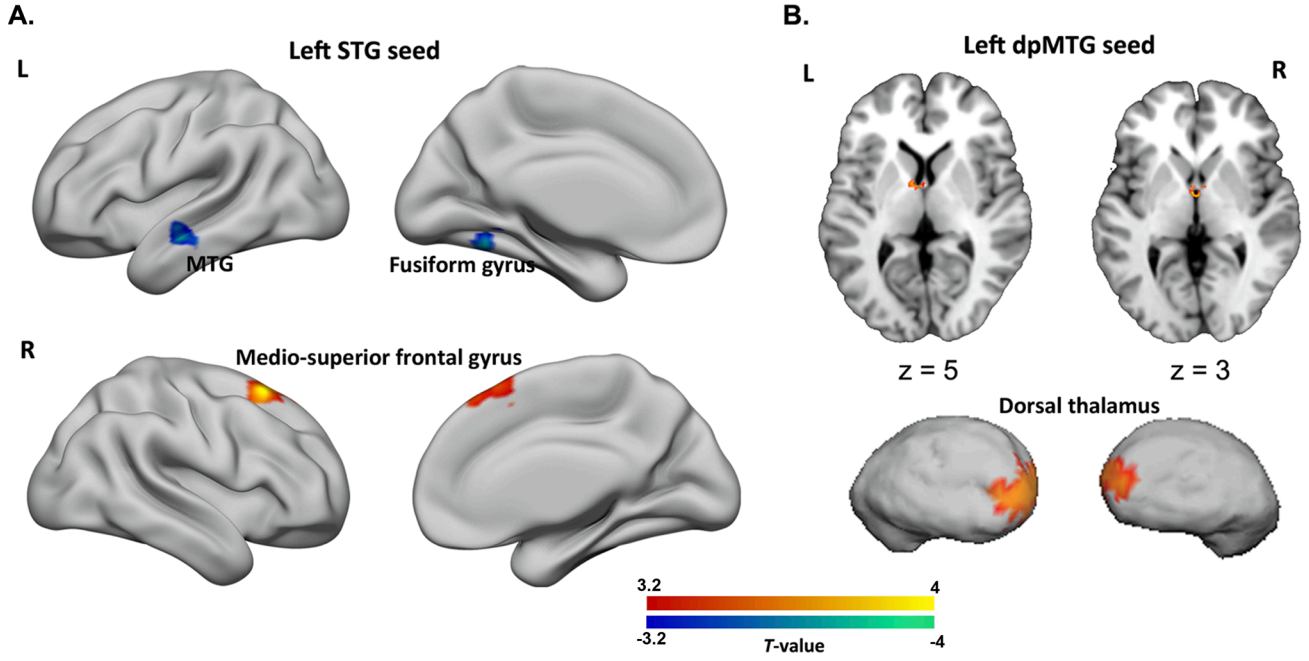

Fig. 2. Differential resting-state functional connectivity (rsFC) with the seed regions in schizophrenia patients compared to healthy subjects. A) For the left STG seed, clusters showing decreased (blue) rsFC for schizophrenia patients were located in the left fusiform gyrus and left middle temporal gyrus, while one cluster in the right medio-superior frontal gyrus showed increased rsFC (red). B) For the left dpMTG seed, we identified one cluster indicating increased rsFC in the bilateral dorsal thalamus of schizophrenia patients, which is displayed on both axial sections and a three-dimensional thalamic surface. The above significant clusters were identified at a cluster-level with family-wise error corrected $p < 0.05$, cluster-forming threshold of $p < 0.001$ at voxel level. L, left; R, right; MFG, middle frontal gyrus; vpMTG, ventral posterior middle temporal gyrus; STG, superior temporal gyrus; dpMTG, dorsal posterior middle temporal gyrus. (For interpretation of the references to color in this figure legend, the reader is referred to the web version of this article.)

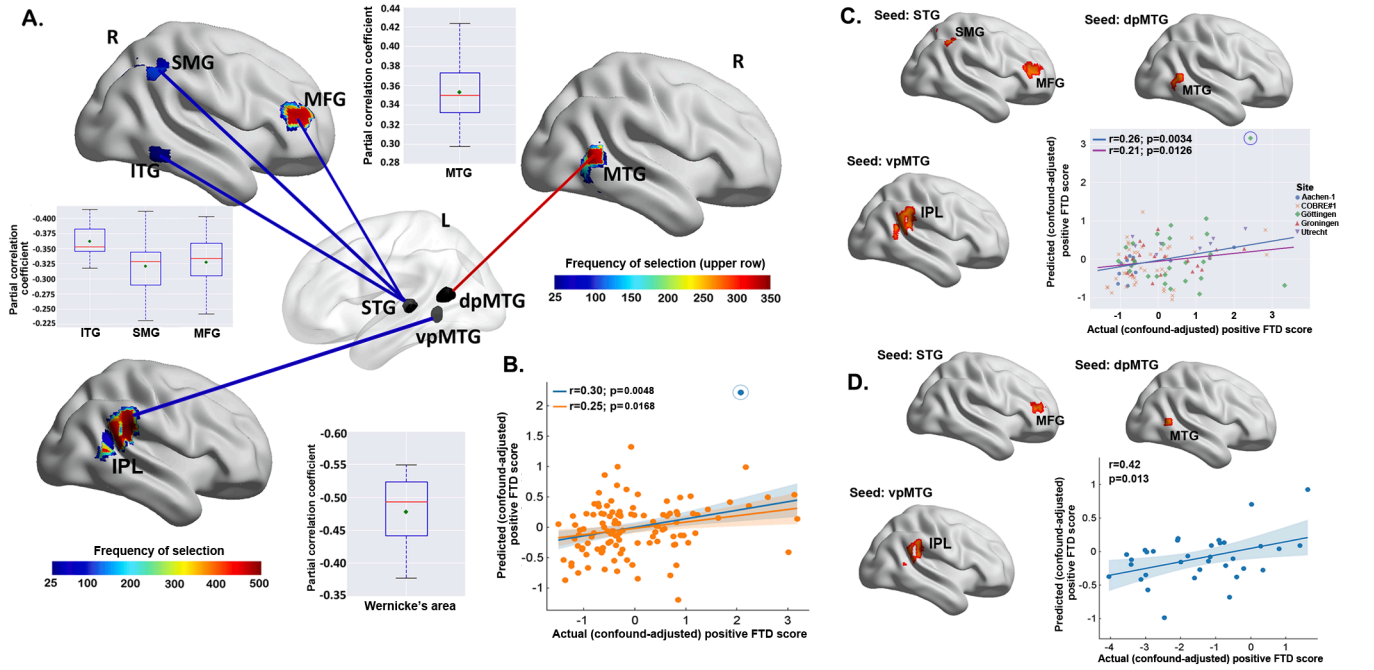

Fig. 3. Cross-validation based feature selection and prediction of individual positive formal thought disorder (FTD) scores from resting-state functional connectivity (rsFC). A) For each seed region and each 10-fold cross-validation, clusters whose rsFC to the seeds that were significantly associated with positive-FTD were accumulated. Mean rsFC values extracted within these clusters were used as features. Frequency of the clusters selected in the overall general linear models conducted on the 500 training samples is color-coded from blue to red. The three seed regions are displayed on a transparent brain. Blue lines indicate negative associations while the red line indicates positive association. Partial correlation coefficients (adjusted for age, gender, and head motion parameters) between the identified significant rsFC patterns and the positive FTD scores, derived from the repeated 10-fold cross-validation, were shown in three boxplots separately for the three seeds (red line depicts the median, green diamond depicts the mean, whiskers represent the 5th and 95th percentiles); B) Scatter shows the Pearson's correlation between the actual (confound-adjusted) positive-FTD scores and their predictions in 10-fold cross-validation within the main sample. The predicted data were the average predictions for each subject across the repeated 10-fold cross-validation runs. The regression line in blue was fitted with the suspected "outlier" (i.e., the circled blue point), while the dark yellow line was fitted after excluding this "outlier"; C) Brain clusters with rsFC to the seeds that were identified as significantly associated with positive FTD scores in leave-one-site-out cross-validation within the main sample. Scatter plots show the correlation between the actual positive-FTD scores and their predictions. The data points were colored differently per site. The regression line in blue was fitted with the suspected "outlier" (i.e., the circled blue point), while the dark yellow line was fitted after excluding this "outlier"; D) Our RVM model, that trained within the main sample based on the rsFC patterns extracted from the three most robustly identified brain clusters, was applied to the independent sample for validation. Scatter plot shows the correlation between the actual positive-FTD scores and their predictions in the independent sample. Shaded areas represent 95% confidence intervals. L, left; R, right; FC, functional connectivity; AT, abstract thinking; FTD, formal thought disorder; STG, superior temporal gyrus; dpMTG, dorsal posterior middle temporal gyrus; vpMTG, ventral posterior middle temporal gyrus; MFG, middle frontal gyrus; SMG, supramarginal gyrus; ITG, inferior temporal gyrus; IPL, inferior parietal lobule. (For interpretation of the references to color in this figure legend, the reader is referred to the web version of this article.)

excluding a suspected outlier of predicted score: $r = 0.21$; $p = 0.0126$; $nRMSE = 1.01$, $p = 0.0388$]; Fig. 3C). In addition, the prediction accuracy (*nRMSE)* did not correlate with the number of subjects in each site ($r = 0.29$, $p = 0.63$; Fig. S1).

We finally validated the predictability of the identified robust rsFC patterns for the positive FTD dimension in an independent sample. In particular, we focused on the clusters located in the right MFG, MTG, and IPL. Clusters in these regions were detected as significantly associated with positive FTD in > 60% of the overall 500 10-fold training samples and also significant in LOSO analyses (Fig. 3D). The extracted rsFC values were used as features for RVM model training within the main sample. After applying the trained model to the validation sample, we found that the actual (confound-adjusted) scores were significantly correlated with the predictions of our model ($r = 0.42$, $p = 0.013$, $nRMSE = 1.32$; Fig. 3D). Lower rsFC between left STG seed and right MFG, and higher rsFC between the left dpMTG and right MTG and between the left vpMTG and right IPL were associated with more-severe positive FTD symptoms.

Additionally, the olanzapine-equivalent dosage of medication did not correlate significantly with the positive FTD dimension score ($r = 0.09$, $p = 0.39$) nor with the rsFC in our data (cluster-level corrected $p < 0.05$), and hence adjusting for olanzapine-equivalent dosage in addition to age, gender, site, and head motion did not alter the predictive patterns. Ten-fold cross-validation revealed that models trained based on the rsFC patterns associated with positive-FTD were not predictive of hallucinations ($r = -0.13$, $p = 0.86$; $nRMSE = 1.08$, $p = 0.61$) and overall symptom severity ($r = 0.05$, $p = 0.21$; $nRMSE = 1.07$, $p = 0.51$), implying the specificity of the positive-FTD associated rsFC patterns in the prediction of the positive FTD dimension in schizophrenia. As shown in Fig. S2, using an alternative denoising approach of ICA-AROMA largely replicated our main results. Furthermore, through the GLMs performed within the main sample implemented as an unsupervised feature selection approach for predictive modeling, we identified multiple clusters showing significant positive or negative rsFC with the three seeds (Fig. S3). These significant clusters, irrespective of which seeds they are connecting, were mainly distributed in precuneus, precentral and temporal regions. Specifically, for the left STG seed, clusters with positive rsFC were located in bilateral sensory-motor cortex and STG/MTG, with negative rsFC located in bilateral middle and superior occipital gyrus as well as right IPL. Clusters significantly connected with the left dpMTG seed were more widely spread, stretching across bilateral frontal, parietal, temporal, precuneus/posterior cingulate cortex, and cerebellar areas. Interestingly, clusters showing positive rsFC with the left vpMTG seed were seated in the lateral hemispheres, while those clusters with negative rsFC were medial. Applying RVM models trained within the main sample using the rsFC patterns of these significantly

connected regions to the validation sample, none of the three FTD dimensions were significantly predicted (positive FTD: $r = 0.25$, $p = 0.145$; negative FTD: $r = -0.13$, $p = 0.480$; composite FTD: $r = -0.05$, $p = 0.765$).

3.3. Functional characterization of the identified brain clusters

Functional profiles for each of the characterized brain clusters, locating in left fusiform gyrus and MTG, right medio-superior, bilateral thalamus, right frontal gyrus MFG, MTG, and IPL, was determined by quantitative forward and reverse inferences on the behavioral domains and paradigm classes as sorted in the BrainMap database (Laird, 2009; Genon et al., 2018). Fig. 4 illustrates separately the results for forward inference (the probability of a special behavioral process relating to activation in a given cluster) and reverse inference (which tests, if a given behavioral process is active, when a particular region is activated). Below, these findings are summarized.

3.3.1. Clusters showing differential rsFC with the seeds in schizophrenia patients compared to healthy controls

The cluster in the left fusiform gyrus was associated with the cognitive domains of speech and memory, together with emotion (anger and fear) and vision perception. The left MTG cluster was primarily associated with language (speech and semantics) and social cognition (theory-of-mind) (Fig. 4A). The cluster in the right medio-superior frontal gyrus was functionally associated with emotion processing (Fig. 4A), while the thalamic cluster was involved in emotion processing (reward and sadness) (Fig. 4B).

3.3.2.

We focused here on the three clusters that were both associated with positive FTD in > 60% of the overall 500 10-fold training samples and significant in LOSO analyses. These three clusters were located in the MFG, MTG, and Wernicke's area. Remarkably, none of these clusters were functionally associated with language-related processes (Fig. 4C). Rather, they were all significantly associated with higher-order cognitive processes, including working memory, social cognition, and executive functions. Specifically, the cluster located in IPL was found as significantly associated with social cognition (theory of mind), executive function and interoception. The MTG cluster was identified as involved in action observation. The cluster located in the MFG was associated

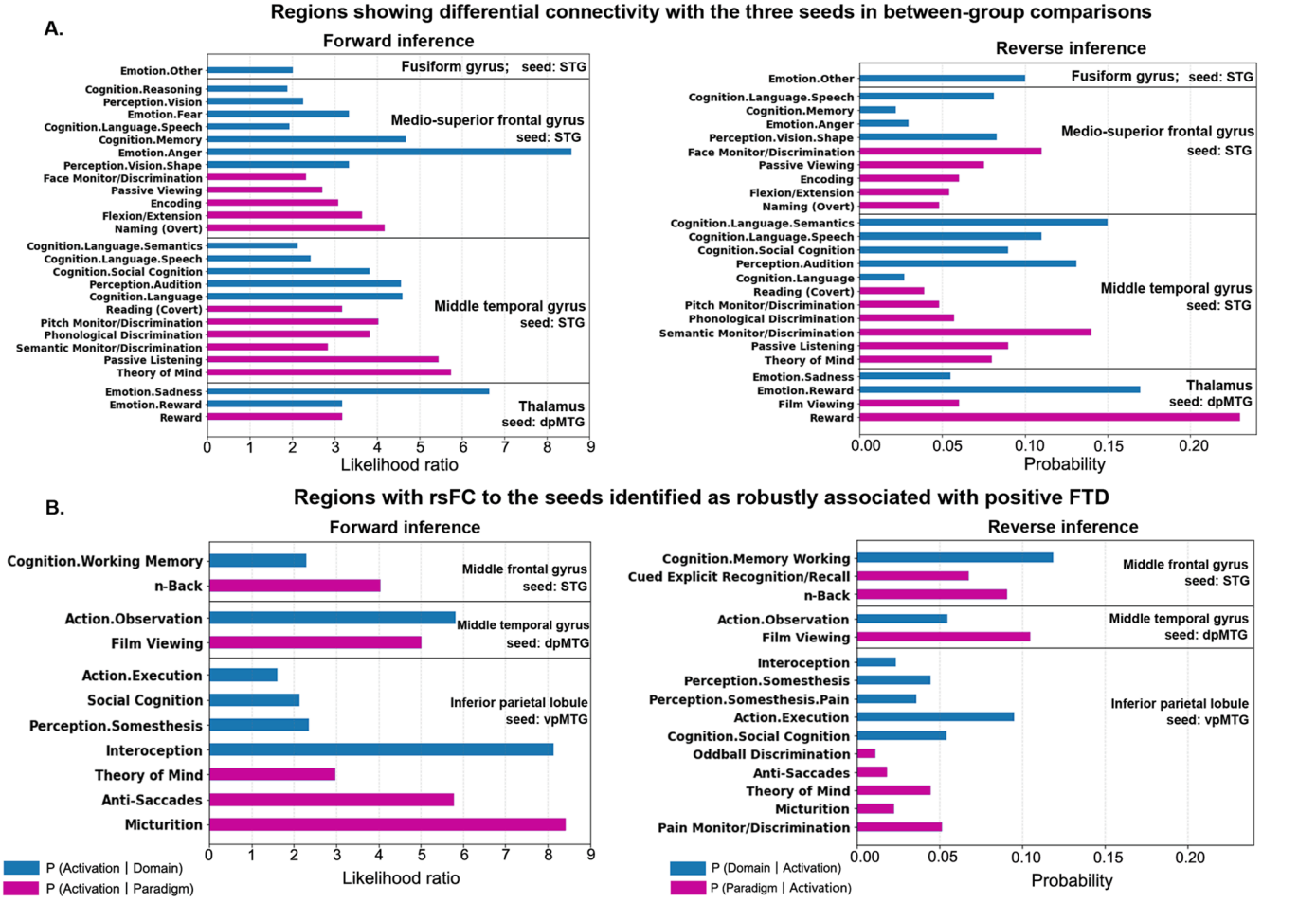

Fig. 4. Functional characterization of the identified brain clusters. Bar charts indicating A) functional profiles of the clusters showing differential resting-state functional connectivity (rsFC) with the two seeds: superior temporal gyrus and dorsal posterior middle temporal gyrus between schizophrenia patients and healthy controls, and B) functional characterization of the brain clusters whose rsFC to the seeds were identified as robustly associated with the severity of positive FTD. Quantitative "forward inference" and "reverse inference" experiments were used to determine the functional profile of each cluster. Regions with significant functional assignments (false discovery rate corrected $p < 0.05$) are presented. The significant activation likelihood ratios for each cluster with respect to a given domain or paradigm (forward inference) and the significant probability of a domain's or paradigm's occurrence given activation in a cluster (reverse inference) are depicted separately. The "P (Activation I Domain/Paradigm)" refers to the activation likelihood (in the forward reference) in a significant region given a particular label (i.e., a behavioral domain or a task paradigm). The "P (Domain I Activation)" refers to the probability of behavioral domains given activation in a particular brain region, which tests for a regions' functional profile based on reverse inference. Similarly, the "P (Paradigm I Activation)" represents the probability of paradigm classes given activation in this particular region. FTD, formal thought disorder; LH, left hemisphere; RH, right hemisphere.

with working memory.

4. Discussion

Our study identified four brain regions showing differential rsFC with the three *meta*-analytically defined FTD-related seeds in schizophrenia patients compared to healthy controls. Following a strict cross-validation procedure (10-fold and LOSO), rsFC patterns of three other regions, implicated in executive functions and higher-order cognitive processes, were identified as robustly associated with the severity of positive FTD across different patient cohorts, sites and scanners. The identified rsFC patterns moreover allowed individual prediction of positive FTD severity in an independent dataset but were not predictive of other positive symptoms, suggesting that these patterns were an individual neurobiological substrate closely related to positive FTD.

Evidence from previous task-based fMRI studies corroborates the notion that the identified brain regions with differential rsFC with the seeds in schizophrenia patients compared to healthy subjects play a role in the pathogenesis of FTD. The fusiform gyrus, e.g., one of the three regions showing differential rsFC with the left STG seed in our study, was reported as hyperactivated during FTD-associated speech production in schizophrenia patients (McGuire et al., 2002). The other region in the right medio-superior frontal gyrus showed increased rsFC to the STG seed, which has been found to exhibit increased neural activity during greater semantic retrieval demands that was significantly correlated with FTD severity in schizophrenia patients (Ragland, 2008). Also the thalamic dorso-medial subfield was identified as differentially connected to the left dpMTG seed. The importance of thalamic abnormalities in the pathophysiology of schizophrenia has been discussed in the context of "cognitive dysmetria", that is, difficulties in gating information, which might result in cognitive deficits on the behavioral level (Andreasen, 1997; Andreasen et al., 1998). The dorso-medial thalamic subfield, in particular, has been implicated in speech processing (Crosson and Hughes, 1987), especially in the retrieval of memory representations in speech perception (Kotz and Schwartze, 2010). On a structural level, the dorso-medial region of thalamus, which mainly projects to the temporal and frontal cortex (Andreasen et al., 1998); shows convergent evidence for structural changes in schizophrenia patients (Behrens, 2003). This further corroborates the hypothesis of dysfunctional fronto-temporo-thalamic networks as a key component in the pathophysiology of schizophrenia (Nickl-Jockschat, 2011; Ellison-Wright et al., 2008), and points towards a possible structure–function-relationship in the thalamus for FTD.

Of note, robust association patterns between rsFC and symptom severity were only found for the positive FTD dimension. In fact, negative FTD symptoms corresponded to three items and the scores of each negative FTD item were not significantly correlated with seed-to-whole-brain rsFC patterns. This indicates that rsFC might be less sensitive in detecting negative than positive FTD. Interestingly, significant clusters from our group comparison on the one hand and our correlation analyses on the other were spatially not overlapping. This seemingly counterintuitive finding, however, is well in line with previous structural MRI findings that showed a similar dissociation between regions implicated in group comparisons and correlations with FTD severity (Sans-Sansa, 2013). Such a dissociation might suggest a distinct subnetwork mediating positive FTD that is neurobiologically largely distinct from the circuits that mediate a general predisposition for FTD (regardless, whether positive or negative). The notion of a global vulnerability mediated by such a network might also explain, why there is no correlation between the composite FTD scores and rsFC.

Remarkably, the identified rsFC patterns were predictive of individual positive-FTD severity in novel patients. Previous findings in the literature on correlations between fMRI parameters and symptom severity so far mostly relied on group level analyses, but fell short to allow individual predictions (Bzdok and Meyer-Lindenberg, 2018), although pioneering predictive studies have successfully identified robust neuromarkers for attention (Rosenberg, 2016) and creative ability (Beaty, 2018) in healthy populations. We would argue that the stably identified (and hence) robust rsFC patterns in repeated cross-validation should constitute a reliable neurobiological substrate of the positive FTD dimension in schizophrenia.

Brain regions whose rsFC with the temporal seeds that identified as robustly associated with positive-FTD were functionally linked to executive and higher-order cognitive processes including working memory and social cognition. Findings from previous task-based fMRI studies implicated abnormal neural activation in brain regions (e.g., the Wernicke's area) involved in the production of coherent speech as essential for positive FTD symptoms in schizophrenia (McGuire et al., 2002; Kircher, 2001a, 2001b). Our own study focused on functional connectivity and implicated a link between positive FTD and brain regions involved in higher-order cognitive processing, thus, extending these previous findings. Previous task-based studies have implicated abnormal neural activations of dorsal prefrontal regions in negative FTD (Kircher, 2003; McGuire, 1998; Fuentes-Claramonte et al.,). Also our results have implicated dorsal prefrontal regions to be associated with positive FTD, however, based on their connectivity patterns, not on their regional activity. These dorsal prefrontal regions are associated with higher order cognitive processes, such as working memory. Our results would strengthen the notion that brain regions involved in executive functioning contribute at least to positive symptom severity. These findings would suggest also a dysexecutive component in positive FTD, while certainly also a dyssemantic contribution seems to be highly relevant. These findings provide new clues to a long-discussed controversy on FTD in schizophrenia (Barrera et al., 2005).

Different from identifying FTD significantly associated regions as a supervised feature selection procedure in predictive modeling, our additional predictive analyses employing an unsupervised approach which selected as features the rsFC patterns of regions showing significant positive or negative rsFC with the seeds, did not reveal a significant prediction of any of the three FTD dimensions in the validation sample. This corroborated the notion in previous studies that supervised feature selection could effectively improve prediction performance. (Shen, 2017) It needs to be cautioned, though, that independent samples, which are not part of the supervised feature selection process, are required for validation, so as to avoid circularity, obtain undistorted statistics, and therefore, valid predictive results. (Kriegeskorte et al., 2009) Comparatively, in unsupervised approaches, the feature selection criteria are not related to the target variable to be predicted, and hence different hypotheses can be raised in addition to supervised predictive modeling as we shown here. Future studies incorporating both the unsupervised and supervised feature selection approaches are encouraged in moving fMRI toward predictive clinical utility in psychiatry.

Several limitations need to be discussed. First, the PANSS, compared to, e.g., the TLC (Kircher et al., 2018), is not a scale that was designed for assessing more fine-grained subcategories of FTD symptoms. However, using relevant items from this widely used and well-established rating scale allows the pooling of data across multiple acquisition sites, and, thus, allows comparisons across populations and different treatment regimens (for a more detailed discussion: Supplementary material S4). Second, the effect size of the correlation between the predicted and actual ratings was moderate. However, despite the clinical complexity of the population and the heterogeneities arising from pooling data from multiple medical centers with different scanners and settings, the current prediction accuracy was similar to those previously reported for predicting, e.g., creativity (Beaty, 2018) and memory performance (Persson et al., 2018), from resting-state data in healthy populations (r-values mostly around 0.2–0.35). Third, there might be concerns regarding potential site effects on prediction. To mitigate this kind of concerns, we first adjusted site effects on both rsFC and FTD dimensions sores within 10-fold cross-validation, and then implemented LOSO which confirmed the 10-fold results. The generated predictive model was, moreover, validated in an independent sample. Also the prediction

accuracy was not site-dependent. We were primarily focusing on the pooled effects and including small sites would add variance to make the analysis more conservative. Forth, we acknowledge that patients were on their regular medication as prescribed by the attending psychiatrists at the time of data acquisition. In general, antipsychotic medication does affect on brain metabolism and blood flow in schizophrenia (Miller, 1997), leading to subsequent BOLD signal changes. However, as antipsychotics are used to target a broad range of positive symptoms (Liemburg et al., 2012), e.g., hallucinations and delusions, and not positive FTD, in specific, medication effects should largely represent a source of random variation when analyzing the neurobiological substrates of FTD in our data. Such noise would effectively obscure robust brain functional associations for FTD, and, in particular, make it harder to train algorithms that work well for out-of-sample prediction of FTD scores. We would argue that the current results should not be driven by medication effects, but rather represent a solid neurobiological basis for the positive FTD in schizophrenia.

To conclude, we here used three *meta*-analytically defined seeds to identify rsFC patterns in schizophrenia patients related to FTD. Associations between rsFC patterns and positive FTD scores we identified were robust that they allowed an individual prediction of symptom severity in patients and, thus, should delineate a robust neurobiological profile for positive FTD. Finally, the positive FTD dimension was found to functionally associate with higher-order cognitive functions, suggesting a dysexecutive contribution to the pathophysiology of positive FTD in schizophrenia.

Declaration of Competing Interest

The authors declare that they have no known competing financial interests or personal relationships that could have appeared to influence the work reported in this paper.

Acknowledgements

We thank the researchers at each of the medical centers for their efforts in recruiting the subjects and sharing the data that made the current work possible. Gratitude is expressed to each of the subjects who spent their time and energy in participating this study and their cooperation. This study was supported by the Deutsche Forschungsgemeinschaft (DFG, EI 816/4-1 to S.B.E.), the National Institute of Mental Health (R01-MH074457 to S.B.E.), the Helmholtz Portfolio Theme “Supercomputing and Modeling for the Human Brain”, the European Union’s Horizon 2020 Research and Innovation Programme under Grant Agreement No. 720270 (HBP SGA1) and 785907 (HBP SGA2), and the Chinese Scholarship Council to J.C.

Author contributions

T.N-J., S.B.E. and J.C. designed the study. J.C. analyzed the data, implemented the machine-learning approaches, and drafted the manuscript. K.R.P., E.C.C. and V.I.M. contributed to the interpretation of the results, and provided technical supports as well as statistical advices. T. W. conducted initial statistical analyses, and provided the meta-analytic brain seed regions. F.H. preprocessed the neuroimaging data. A.A., B.D., O.G., R.J., L.K. and I.E.S. acquired and provided the multi-site data. All authors participated in the interpretation of the results, critical revision of the manuscript for important intellectual content, and read and approved the manuscript.

Code availability

The code for seed connectome-based predictive modeling can be found at https://github.com/jichen-psy/Seed-commectome-based-predictive-modeling.

Appendix A. Supplementary data

Supplementary data to this article can be found online at https://doi.org/10.1016/j.nicl.2021.102666.

References

Altman, Naomi, Krzywinski, Martin, 2016. Analyzing outliers: influential or nuisance? Nat. Meth. 13 (4), 281–282.
Andreasen, N.C., 1979. Thought, language, and communication disorders: II diagnostic significance. *Arch. Gen. Psychiatry* 36 (12), 1325. https://doi.org/10.1001/archpsyc.1979.01780120055007.
Andreasen, N.C., 1986. Scale for the assessment of thought, language, and communication (TLC). Schizophr. Bull. 12 (3), 473–482.
Andreasen, Nancy C, 1997. The role of the thalamus in schizophrenia. Can. J. Psychiatry 42 (1), 27–33.
Andreasen, N.C., Flaum, M., Swayze, V.W., Tyrrell, G., Arndt, S., 1990. Positive and negative symptoms in schizophrenia: a critical reappraisal. Arch. Gen. Psychiatry 47, 615–621.
Andreasen, N.C., Paradiso, S., O’leary,, D., S., 1998. “Cognitive dysmetria” as an integrative theory of schizophrenia: a dysfunction in cortical-subcortical-cerebellar circuitry? Schizophr. Bull. 24, 203–218.
Arcuri, S.M., Broome, M.R., Giampietro, V., Amaro, E., Kircher, T.T.J., Williams, S.C.R., Andrew, C.M., Brammer, M., Morris, R.G., McGuire, P.K., 2012. Faulty suppression of irrelevant material in patients with thought disorder linked to attenuated frontotemporal activation. Schizophr. Res. Treatment 2012, 1–12.
Armando, M., Pontillo, M., De Crescenzo, F., Mazzone, L., Monducci, E., Lo Cascio, N., Santonastaso, O., Pucciarini, M.L., Vicari, S., Schimmelmann, B.G., Schultze-Lutter, F., 2015. Twelve-month psychosis-predictive value of the ultra-high risk criteria in children and adolescents. Schizophr. Res. 169 (1-3), 186–192.
Barrera, A., McKenna, P., Berrios, G., 2005. Formal thought disorder in schizophrenia: an executive or a semantic deficit? Psychol. Med. 35, 121–132.
Beaty, R.E., et al., 2018. Robust prediction of individual creative ability from brain functional connectivity. Proc. Natl. Acad. Sci. U. S. A. 115, 1087–1092.
Beaty, R.E., Kenett, Y.N., Christensen, A.P., Rosenberg, M.D., Benedek, M., Chen, Q., Fink, A., Qiu, J., Kwapil, T.R., Kane, M.J., Silvia, P.J., 2018. Robust prediction of individual creative ability from brain functional connectivity. Proc. Natl. Acad. Sci. U. S. A. 115 (5), 1087–1092.
Behrens, T.E., et al., 2003. Non-invasive mapping of connections between human thalamus and cortex using diffusion imaging. Nat. Neurosci. 6, 750–757.
Bzdok, D., Meyer-Lindenberg, A., 2018. Machine learning for precision psychiatry: opportunities and challenges. Biol. Psychiatry *Cogn. Neurosci. Neuroim.* 3, 223–230.
Cavelti, M., Kircher, T., Nagels, A., Strik, W., Homan, P., 2018. Is formal thought disorder in schizophrenia related to structural and functional aberrations in the language network? A systematic review of neuroimaging findings. Schizophr. Res. 199, 2–16.
Chen, J., et al., 2020. Neurobiological divergence of the positive and negative schizophrenia subtypes identified on a new factor structure of psychopathology using non-negative factorization: an international machine learning study. Biol. Psychiatry 87, 282–293.
Chen, J., et al., 2021. Intrinsic connectivity patterns of task-defined brain networks allow individual prediction of cognitive symptom dimension of schizophrenia and are linked to molecular architecture. Biol. Psychiatry 89, 308–319.
Chen, P.J., Fan, L.Y., Hwang, T.J., Hwu, H.G., Liu, C.M., Chou, T.L., 2014. The deficits on a cortical–subcortical loop of meaning processing in schizophrenia. Neuroreport 24, 147–151.
Cieslik, E.C., et al., 2012. Is there “one” DLPFC in cognitive action control? Evidence for heterogeneity from co-activation-based parcellation. Cereb. Cortex. 23, 2677–2689.
Ciric, Rastko, Rosen, Adon F.G., Erus, Guray, Cieslak, Matthew, Adebimpe, Azeez, Cook, Philip A., Bassett, Danielle S., Davatzikos, Christos, Wolf, Daniel H., Satterthwaite, Theodore D., 2018. Mitigating head motion artifact in functional connectivity MRI. Nat. Protoc. 13 (12), 2801–2826.
Clos, Mareike, Amunts, Katrin, Laird, Angela R., Fox, Peter T., Eickhoff, Simon B., 2013. Tackling the multifunctional nature of Broca’s region meta-analytically: co-activation-based parcellation of area 44. NeuroImage 83, 174–188.
Combrisson, E., Jerbi, K., 2015. Exceeding chance level by chance: the caveat of theoretical chance levels in brain signal classification and statistical assessment of decoding accuracy. J. Neurosci. Methods 250, 126–136.
Crosson, B., Hughes, C.W., 1987. Role of the thalamus in language: Is it related to schizophrenic thought disorder? Schizophr. Bull. 13 (4), 605–621.
DeLisi, L.E., 2001. Speech disorder in schizophrenia: review of the literature and exploration of its relation to the uniquely human capacity for language. Schizophr. Bull. 27 (3), 481–496.
DeVylder, J.E., Muchomba, F.M., Gill, K.E., Ben-David, S., Walder, D.J., Malaspina, D., Corcoran, C.M., 2014. Symptom trajectories and psychosis onset in a clinical high risk cohort: the relevance of subthreshold thought disorder. Schizophr. Res. 159 (2-3), 278–283.
Dong, D., et al., 2018. Dysfunction of large-scale brain networks in schizophrenia: a meta-analysis of resting-state functional connectivity. Schizophr. Bull. 44, 168–181.
Dubois, J., et al., 2018. A distributed brain network predicts general intelligence from resting-state human neuroimaging data. Philos. Trans. R. Soc. Lond. B. Biol. Sci. 373, 20170284.
Eickhoff, S.B., Bzdok, D., Laird, A.R., Kurth, F., Fox, P.T., 2012. Activation likelihood estimation revisited. Neuroimage 59, 2349–2361.

Ellison-Wright, I., Glahn, D.C., Laird, A.R., Thelen, S.M., Bullmore, E., 2008. The anatomy of first-episode and chronic schizophrenia: an anatomical likelihood estimation meta-analysis. Am. J. Psychiatry 165, 1015–1023.
Finn, E.S., Shen, X., Scheinost, D., Rosenberg, M.D., Huang, J., Chun, M.M., Papademetris, X., Constable, R.T., 2015. Functional connectome fingerprinting: identifying individuals using patterns of brain connectivity. Nat. Neurosci. 18 (11), 1664–1671.
Fox, M.D., Raichle, M.E., 2007. Spontaneous fluctuations in brain activity observed with functional magnetic resonance imaging. Nat. Rev. Neurosci. 8 (9), 700–711.
Friederici, A.D., 2012. The cortical language circuit: from auditory perception to sentence comprehension. Trends. Cogn. Sci. 16 (5), 262–268.
Fuentes-Claramonte, P. et al. Brain functional correlates of formal thought disorder in schizophrenia: examining the frontal/dysexecutive hypothesis. Psychol. Med. (2020) https://doi.org/10.1017/S0033291720001063.
Gardner, D.M., Murphy, A.L., O'Donnell, H., Centorrino, F., Baldessarini, R.J., 2010. International consensus study of antipsychotic dosing. Am. J. Psychiatry 167, 686–693.
Genon, S., et al., 2017. The right dorsal premotor mosaic: organization, functions, and connectivity. Cereb. Cortex. 27, 2095–2110.
Genon, S., Reid, A., Langner, R., Amunts, K., Eickhoff, S.B., 2018. How to characterize the function of a brain region. Trends. Cogn. Sci. 22, 350–364.
Goldberg, T.E., Aloia, M.S., Gourovitch, M.L., Missar, D., Pickar, D., Weinberger, D.R., 1998. Cognitive substrates of thought disorder, I: the semantic system. Am. J. Psychiatry 155, 1671–1676.
Griffanti, L., Salimi-Khorshidi, G., Beckmann, C.F., Auerbach, E.J., Douaud, G., Sexton, C. E., Zsoldos, E., Ebmeier, K.P., Filippini, N., Mackay, C.E., Moeller, S., Xu, J., Yacoub, E., Baselli, G., Ugurbil, K., Miller, K.L., Smith, S.M., 2014. ICA-based artefact removal and accelerated fMRI acquisition for improved resting state network imaging. Neuroimage 95, 232–247.
Guo, Jianhua, Huang, Wei, Williams, Billy M., 2015. Real time traffic flow outlier detection using short-term traffic conditional variance prediction. Transp. Res. Part C. 50, 160–172.
Guyon, I., Elisseeff, A., 2003. An introduction to variable and feature selection. J. Mach. Learn. Res. 3, 1157–1182.
Hartmann, J.A., et al., 2016. Declining transition rates to psychotic disorder in "ultra-high risk" clients: investigation of a dilution effect. Schizophr. Res. 170, 130–136.
Horn, H., Federspiel, A., Wirth, M., Müller, T.J., Wiest, R., Walther, S., Strik, W., 2010. Gray matter volume differences specific to formal thought disorder in schizophrenia. Psychiatry Res. Neuroim. 182 (2), 183–186.
Kay, S.R., Fiszbein, A., Opler, L.A., 1987. The positive and negative syndrome scale (PANSS) for schizophrenia. Schizophr. Bull. 13 (2), 261–276.
Kircher, T.T., et al., 2001aa. Differential activation of temporal cortex during sentence completion in schizophrenic patients with and without formal thought disorder. Schizophr. Res. 50, 27–40.
Kircher, T.T., et al., 2001bb. Neural correlates of formal thought disorder in schizophrenia: preliminary findings from a functional magnetic resonance imaging study. Arch. Gen. Psychiatry 58, 769–774.
Kircher, T., et al., 2003. Neural correlates of" negative" formal thought disorder. Der. Nervenarzt. 74, 748–754.
Kircher, T., Bröhl, H., Meier, F., Engelen, J., 2018. Formal thought disorders: from phenomenology to neurobiology. Lancet Psychiatry 5 (6), 515–526.
Kircher, T., Whitney, C., Krings, T., Huber, W., Weis, S., 2008. Hippocampal dysfunction during free word association in male patients with schizophrenia. Schizophr. Res. 101, 242–255.
Kohavi, R., John, G.H., 1997. Wrappers for feature subset selection. Artif. Intell. 97 (1-2), 273–324.
Kotz, Sonja A., Schwartze, Michael, 2010. Cortical speech processing unplugged: a timely subcortico-cortical framework. Trends. Cogn. Sci. 14 (9), 392–399.
Kraguljac, N.V., et al., 2017. Ketamine modulates hippocampal neurochemistry and functional connectivity: a combined magnetic resonance spectroscopy and resting-state fMRI study in healthy volunteers. Mol. Psychiatry 22, 562–569.
Kriegeskorte, Nikolaus, Simmons, W Kyle, Bellgowan, Patrick S F, Baker, Chris I, 2009. Circular analysis in systems neuroscience: the dangers of double dipping. Nat. Neurosci. 12 (5), 535–540.
Laird, A.R., et al., 2009. ALE meta-analysis workflows via the brainmap database: progress towards a probabilistic functional brain atlas. Front. Neuroinform. 3, 23.
Lehmann, Rüdiger, 2013. 3 σ-rule for outlier detection from the viewpoint of geodetic adjustment. J. Surv. Eng. 139 (4), 157–165.
Liemburg, E.J., et al., 2012. Abnormal connectivity between attentional, language and auditory networks in schizophrenia. Schizophr. Res. 135, 15–22.
Edith J. Liemburg Henderikus Knegtering Hans C. Klein Rudie Kortekaas André Aleman Antipsychotic medication and prefrontal cortex activation: a review of neuroimaging findings Eur. Neuropsychopharmacol. 22 6 2012 387 400.
Liu, X., Eickhoff, S.B., Hoffstaedter, F., Genon, S., Caspers, S., Reetz, K., Dogan, I., Eickhoff, C.R., Chen, J.i., Caspers, J., Reuter, N., Mathys, C., Aleman, A., Jardri, R., Riedl, V., Sommer, I.E., Patil, K.R., 2020. Joint multi-modal parcellation of the human striatum: functions and clinical relevance. Neurosci. Bull. 36 (10), 1123–1136.
McGuire, P.K., et al., 1998. Distinct neural correlates of 'positive' and 'negative' thought disorder. Schizophr. Res. 1, 111.
McGuire, P., Quested, D., Spence, S., Murray, R., Frith, C., Liddle, P., 2002. Pathophysiology of 'positive' thought disorder in schizophrenia. Br. J. Psychiatry 173, 231–235.
Miller, D.D., et al., 1997. Effect of antipsychotics on regional cerebral blood flow measured with positron emission tomography. Neuropsychopharmacology 17, 230–240.
More, S., Eickhoff, S. B., Julian, C., Patil, K. R. Confound Removal and Normalization in Practice: A Neuroimaging Based Sex Prediction Case Study. Preprint available at https://juser.fz-juelich.de/record/877721; Accepted in the European Conference on Machine Learning and Principles and Practice of Knowledge Discovery in Databases (ECML PKDD; https://ecmlpkdd2020.net/programme/ accepted/#ADSTab) (2020).
Murphy, K., Fox, M.D., 2017. Towards a consensus regarding global signal regression for resting state functional connectivity MRI. Neuroimage 154, 169–173.
Nagels, A., et al., 2012. Effects of ketamine-induced psychopathological symptoms on continuous overt rhyme fluency. Eur. Arch. Psychiatry Clin. Neurosci. 262, 403–414.
Nagels, A., et al., 2016. Distinct neuropsychological correlates in positive and negative formal thought disorder syndromes: the thought and language disorder scale in endogenous psychoses. Neuropsychobiol. 73, 139–147.
Nickl-Jockschat, T., et al., 2011. Progressive pathology is functionally linked to the domains of language and emotion: meta-analysis of brain structure changes in schizophrenia patients. Eur. Arch. Psychiatry Clin. Neurosci. 261, 166–171.
Noirhomme, Q., et al., 2014. Biased binomial assessment of cross-validated estimation of classification accuracies illustrated in diagnosis predictions. Neuroim. Clin. 4, 687–694.
Ott, S., Roberts, S., Rock, D., Allen, J., Erlenmeyer-Kimling, L., 2002. Positive and negative thought disorder and psychopathology in childhood among subjects with adulthood schizophrenia. Schizophr. Res. 58, 231–239.
Parkes, Linden, Fulcher, Ben, Yücel, Murat, Fornito, Alex, 2018. An evaluation of the efficacy, reliability, and sensitivity of motion correction strategies for resting-state functional MRI. Neuroimage 171, 415–436.
Persson, Jonas, Stening, Eva, Nordin, Kristin, Söderlund, Hedvig, 2018. Predicting episodic and spatial memory performance from hippocampal resting-state functional connectivity: evidence for an anterior-posterior division of function. Hippocampus 28 (1), 53–66.
Pervaiz, U., Vidaurre, D., Woolrich, M.W., Smith, S.M., 2020. Optimising network modelling methods for fMRI. NeuroImage 211, 116604. https://doi.org/10.1016/j.neuroimage.2020.116604.
Pettersson-Yeo, W., Allen, P., Benetti, S., McGuire, P., Mechelli, A., 2011. Dysconnectivity in schizophrenia: where are we now? Neurosci. Biobehav. Rev. 35, 1110–1124.
Power, J.D., Barnes, K.A., Snyder, A.Z., Schlaggar, B.L., Petersen, S.E., 2012. Spurious but systematic correlations in functional connectivity MRI networks arise from subject motion. NeuroImage 59 (3), 2142–2154.
Power, J.D., Schlaggar, B.L., Petersen, S.E., 2015. Recent progress and outstanding issues in motion correction in resting state fMRI. Neuroimage 105, 536–551.
Pruim, Raimon H.R., Mennes, Maarten, van Rooij, Daan, Llera, Alberto, Buitelaar, Jan K., Beckmann, Christian F., 2015. ICA-AROMA: A robust ICA-based strategy for removing motion artifacts from fMRI data. NeuroImage 112, 267–277.
Ragland, J.D., et al., 2008. Effect of retrieval effort and switching demand on fMRI activation during semantic word generation in schizophrenia. Schizophr. Res. 99, 312–323.
Roche, E., et al., 2016. The prognostic value of formal thought disorder following first episode psychosis. Schizophr. Res. 178, 29–34.
Roche, E., Creed, L., MacMahon, D., Brennan, D., Clarke, M., 2015. The epidemiology and associated phenomenology of formal thought disorder: a systematic review. Schizophr. Bull. 41, 951–962.
Rosenberg, M.D., et al., 2016. A neuromarker of sustained attention from whole-brain functional connectivity. Nat. Neurosci. 19, 165–171.
Rosenberg, M.D., Finn, E.S., Scheinost, D., Papademetris, X., Shen, X., Constable, R.T., Chun, M.M., 2016. A neuromarker of sustained attention from whole-brain functional connectivity. Nat. Neurosci. 19 (1), 165–171.
Salimi-Khorshidi, G., Douaud, G., Beckmann, C.F., Glasser, M.F., Griffanti, L., Smith, S. M., 2014. Automatic denoising of functional MRI data: combining independent component analysis and hierarchical fusion of classifiers. NeuroImage 90, 449–468.
Sans-Sansa, B., et al., 2013. Association of formal thought disorder in schizophrenia with structural brain abnormalities in language-related cortical regions. Schizophr. Res. 146, 308–313.
Shen, X., et al., 2017. Using connectome-based predictive modeling to predict individual behavior from brain connectivity. Nat. Protoc. 12, 506–518.
Skudlarski, P., et al., 2010. Brain connectivity is not only lower but different in schizophrenia: a combined anatomical and functional approach. Biol. Psychiatry 68, 61–69.
Smith, S.M., Nichols, T.E., 2018. Statistical challenges in "big data" human neuroimaging. Neuron 97 (2), 263–268.
Snoek, L., Miletić, S., Scholte, H.S., 2019. How to control for confounds in decoding analyses of neuroimaging data. NeuroImage 184, 741–760.
Tan, E.J., Thomas, N., Rossell, S.L., 2014. Speech disturbances and quality of life in schizophrenia: differential impacts on functioning and life satisfaction. Compr. Psychiatry 55 (3), 693–698.
Tipping, M.E., 2001. Sparse Bayesian learning and the relevance vector machine. J. Mach. Learn. Res. 1, 211–244.
Uhlhaas, P.J., 2013. Dysconnectivity, large-scale networks and neuronal dynamics in schizophrenia. Curr. Opin. Neurobiol. 23 (2), 283–290.
Wensing, T., et al., 2017. Neural correlates of formal thought disorder: an activation likelihood estimation meta-analysis. Hum. Brain Mapp. 38, 4946–4965.
Yang, G.J., Murray, J.D., Repovs, G., Cole, M.W., Savic, A., Glasser, M.F., Pittenger, C., Krystal, J.H., Wang, X.-J., Pearlson, G.D., Glahn, D.C., Anticevic, A., 2014. Altered global brain signal in schizophrenia. Proc. Natl. Acad. Sci. U. S. A. 111 (20), 7438–7443.
Yarkoni, T.Big correlations in little studies: Inflated fMRI correlations reflect low statistical power-Commentary on Vul, et al. Perspect Psychol. Stud. 4 2009 294 298.